Radio Science

RESEARCH ARTICLE
10.1029/2018RS006680

Key Points:
- Lightning generates the required signal needed for ionospheric specification
- The ionograms presented here are the first to be derived from lightning measurements
- Measurements are not subject to frequency restrictions

Correspondence to:
K. S. Obenberger,
obenken@icloud.com

Citation:
Obenberger, K. S., Dowell, J. D., Malins, J. B., Parris, R., Pedersen, T., & Taylor, G. B. (2018). Using lightning as a HF signal source to produce ionograms. *Radio Science*, *53*, 1419–1425. https://doi.org/10.1029/2018RS006680

Received 9 JUL 2018
Accepted 30 OCT 2018
Accepted article online 4 NOV 2018
Published online 13 NOV 2018

Using Lightning as a HF Signal Source to Produce Ionograms

K. S. Obenberger[1], J. D. Dowell[2], J. Malins[2], R. T. Parris[1], T. R. Pedersen[1], and G. B. Taylor[2]

[1]Space Vehicles Directorate, Air Force Research Laboratory, Kirtland AFB, NM, USA, [2]Department of Physics and Astronomy, University of New Mexico, Albuquerque, NM, USA

Abstract Modern techniques for specifying the ionosphere include the use of ionosondes, which both transmit and receive sweep soundings in the high-frequency (HF) band. We replicate this process by observing the broad band emission from lightning using the Long Wavelength Array, Sevilleta, radio telescope. We use this station to observe the powerful broadband radio bursts from the breakdown of air that occurs during lightning flashes. For nearby lightning we observe both the direct line of sight and the delayed ionospheric reflection. By correlating the amplitude time series from the direct line of sight to that of the ionospheric reflection, we can accurately measure the group delay as a function of frequency. By separating into right-hand circular and left-hand circular, we can derive both the O mode and X mode ionograms. This novel technique allows for accurate ionograms to be made even in restricted frequency bands and provides a means to probe density profiles at multiple locations of the ionosphere on short time scales with a single receiver station.

Plain Language Summary In this paper, we present a novel technique that leverages the natural radio emissions from lightning as a signal source to measure the electron density profile of the bottomside ionosphere. Such profile measurements are known as ionograms. Previous methods to produce ionograms make use of RADAR systems composed of both a transmitter and receiver. Our method, however, requires only a receiver placed in proximity to ongoing lightning storms. These measurements are the first of their kind to use naturally occurring radio emission to produce ionograms. This work opens the door to further research, where scattered storms could provide key measurements for specifying the spatial and temporal structure present within the ionosphere.

1. Introduction

For vertical soundings of the ionosphere, the local plasma frequency sets the maximum transmitted frequency at a given altitude. All frequencies below the plasma frequency will be reflected back to Earth, and the plasma frequency is proportional to $\sqrt{n_e}$, where n_e is the electron density. A broad range of radio frequencies is required to probe the electron density profile of the ionosphere. The range of electron densities for the bulk of the ionosphere are within the medium-frequency (0.3–3 MHz) and high-frequency (HF; 3–30 MHz) bands.

The ionosphere is broken up into three layers, which are known as the *D* (60–90 km), *E* (90–150 km), and *F* (150–500 km) layers. Generally speaking, the electron density of the ionosphere increases as a function of altitude; therefore, higher frequencies will be reflected at higher altitudes. That is, until the peak density in the *F* layer is reached at which point the electron density decreases. Above the *F* layer peak no vertically transmitted signals are reflected back to Earth. Furthermore, the *F* layer is often broken up into the *F*1 and *F*2 layers.

The group delay as a function of frequency for a sounding measurement provides the information to reconstruct the electron density profile of the bottomside ionosphere. Perhaps the most important frequencies to measure are the peaks of the respective *E*, *F*1, and *F*2 layers (fofE, foF1, and foF2).

A group delay measurement of the ionosphere is called an ionogram and is typically produced by an ionosonde or a digisonde (digital ionosonde), which transmits and receives soundings that sweep through the HF band. Figure 1 shows an ionogram made using a Digisonde Portable System 4-D (DPS-4D; Reinisch et al., 2008) at Kirtland Air Force Base (KAFB). In this case, the ordinary wave (O mode) group delay at each frequency, shown in red, is traced and modeled using the automatic ionogram scaling system (ARTIST; Reinisch

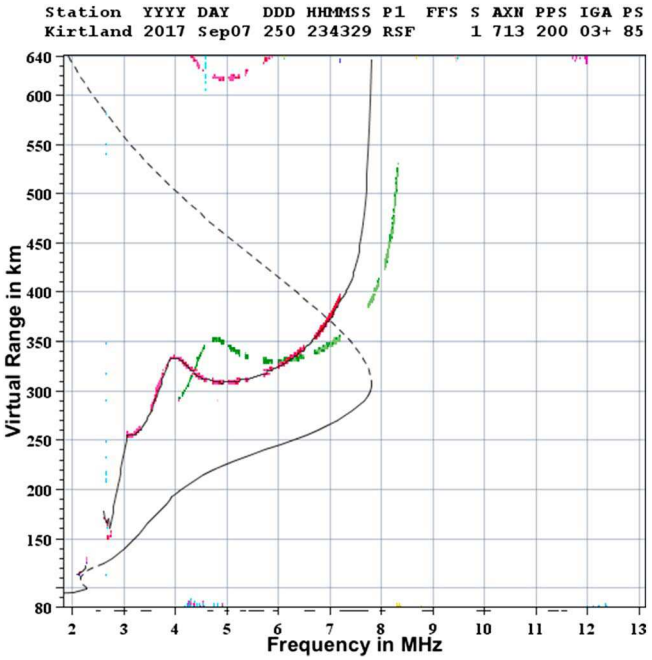

Figure 1. An ionogram created by the Digisonde Portable System 4-D at Kirtland Air Force Base on 7 September 2017. Group delays of O mode (ordinary wave) returns are shown in red, and X mode (extraordinary wave) returns are shown in green. A modeled trace of the O mode returns are shown with a black line following the group delay and the ARTIST estimated plasma frequency as a function of height is shown in a solid curve peaking at ~7.83 MHz at ~300 km. A two hop echo can also be seen above 600 km. Many gaps are present in the data where frequency restrictions exist. Most notably there is a large gap between 7.1 and 7.8 MHz, precisely where the O mode foF2 would be.

& Huang, 1983). ARTIST models this trace and constructs an estimate of the plasma frequency as a function of height.

A single ionosonde can only produce vertical soundings and gets limited angular information, so it misses some detailed characteristics of spatial structure such as traveling ionospheric disturbances (TIDs) or the patchy nature of the *E* region. The temporal structure of TIDs can be ascertained by performing soundings over a long period of time, and multiple reflection points can provide additional information. The propagation geometry from a single monostatic system is not ideal for wide area TID characterization. Pairs of ionosondes can be tuned to listen for oblique returns from each other, and a network of many nearby ionosondes could correlate signals and resolve TID structure. However, the expense of equipment, the real-estate and power requirements for transmitters/receivers, and the trouble of getting transmit licensure have resulted in the lack of wide spread use of such networks.

Another issue facing ionosondes is that it can take several minutes to sweep through all of the necessary frequencies to make an ionogram with sufficient signal-to-noise (SNR) ratio at all frequencies. Since the ionosphere is dynamic on these timescales, the ionogram does not represent a true instantaneous profile. Moreover, many frequency bands are restricted; this creates gaps in the usable spectrum for HF sounding. These gaps, which can be sizable, can significantly degrade the ability to automatically or manually scale the resulting ionogram. If key ionospheric plasma frequencies such as foF1 or foF2 are within a restricted band, the estimated density profile could be severely affected.

It would be advantageous to seek out natural signals that can be used as HF sounders. While many natural phenomena emit RFs, few are powerful enough for ionospheric sounding. Lightning, however, provides powerful, broadband radio emission at the necessary frequencies and is common in many parts of the world. In fact, for the past two decades, ionospheric scientists have been using RF emissions from lightning to probe the ionosphere. These techniques, however, have only made use of the lowest frequency components to observe the bottommost of the *D* region (Cummer et al., 1998; Jacobson et al., 2007, 2008). Such observations leverage the extremely powerful burst of radio emission that is generated as current flows in a cloud-to-ground lightning (CG) return stroke. The bulk of this emission occurs below the low-frequency band (< 300 kHz) and can be as powerful as a few gigawatts. It is very difficult to produce such powerful emission at these frequencies with man-made devices. Since *D* layer reflections require frequencies below ~ 1 MHz, lightning has become a preferred signal of opportunity.

While soundings of the *D* layer are best done below 1 MHz, the denser *E* and *F* layers typically require soundings in the HF and sometimes even very high frequency (VHF; 30–300 MHz) bands. The RF emissions from CG return strokes are not powerful enough at these frequencies to be used as an HF ionospheric sounder. However, very powerful broadband bursts in the HF-VHF bands are generated by the electrical breakdown of air during intracloud (IC) and CG flashes. The breakdown process has been well studied by VHF imagers using both time of arrival (Proctor, 1981; Proctor et al., 1981; Rison et al., 1999; Thomas et al., 2004) and interferometry (Rhodes et al., 1994; Shao & Krehbiel, 1996; Shao & Rhodes, 1996; Shao et al., 1995). While the physics of the HF/VHF emission process during breakdown is of high scientific value, a detailed discussion is unnecessary for the purpose of this paper. Rather, it is sufficient to say that for a single lightning flash the breakdown process produces a unique waveform comprised of hundreds of short duration (~ 1–100 μs) spark-like bursts across the HF and VHF bands. These bursts occur over the entire duration of a flash, which can last anywhere between ~ 100 ms and ~ 1 s.

For HF/VHF studies of the ionosphere, lightning is considered a large source of interference. For instance, when an ionosonde is sweeping through the HF spectrum, each burst of nearby lightning will produce a *source* at a spurious range, thus adding to the noise of a measurement. However, where there is interference there may also be opportunity. The ionosphere will impart the same dispersion signal onto a short broadband pulse as it

Table 1
Observation Details

Date (YYYY/MM/DD)	Start time (UT)	Duration (hours)	foF2 (MHz)
2017/08/29	21:05:16	1.0	5.8–6.1
2017/09/06	21:41:45	1.5	6.0–6.2
2017/09/07	22:40:14	1.0	7.2–8.0

does to an ionosonde sweep. Therefore, a broadband receiver situated to detect both the direct line-of-sight and the ionospheric reflection of lightning could produce ionograms without the need for any transmissions.

During the late summer monsoon season in New Mexico, afternoon lightning storms are common and widespread, providing a reliable test bed for creating ionograms from lightning HF emissions. The Long Wavelength Array, Sevilleta (LWA-SV), a radio telescope located in central New Mexico (Cranmer et al., 2017), capable of observing between 3 and 88 MHz, is optimally situated to observe lightning across the HF and VHF bands. In this paper we report on a successful experiment to make ionograms from LWA-SV observations of lightning.

2. LWA-SV Observations

LWA-SV is the second 256 element station of the larger conceived 52 station LWA and uses the same dual polarization antennas and similar layout to the first LWA station (LWA1), which is located 75 km to the southwest (Ellingson et al., 2013). LWA-SV differs from LWA1 in that the analog filters have been modified to allow observations down to 3 MHz, whereas the LWA1 has a steep cutoff below 10 MHz. LWA-SV also differs from LWA1 in the digital signal processing design, which is based on the Reconfigurable Open Architecture Computing Hardware version 2 boards and GPU servers employing the Bifrost framework (Cranmer et al., 2017). LWA-SV is capable of recording 100 kHz continuously from all antennas, recording 5-s snapshots of up to 20 MHz from all antennas, or recording up to 20 MHz of continuous beamformed data. With 256 dual polarization antennas and broadband capabilities, LWA-SV brings unprecedented sensitivity to ionospheric research.

For such an experiment we would ideally collect broadband data from all antennas, which would allow for imaging and direction finding. However, the current cadence for this mode is 5 s every $\sim$ 15 min, which is too slow to ensure reliable observations. A future upgrade will hopefully reduce this cadence to a sufficient level of down to $\sim$ 1 min and potentially allow self triggering off of lightning to reduce data rate. As a first attempt to create ionograms from HF lightning emissions, we used the broadband capabilities of the LWA-SV beamformer. At the time of this experiment the beamformer was limited to a single beam with two tunings. With an in-phase and quadrature (IQ) sampling rate of 10 MS/s, each tuning can be set to any particular center frequency and receive $\pm$ 5 MHz.

We observed in the afternoon on three separate days during the 2017 monsoon season, when storms were observed in the area. Table 1 shows the date, time, and duration of the observations as well as the range in *F*2 layer peak plasma frequency (foF2) as observed by a DPS-4D colocated with LWA-SV and nearby DPS-4D at KAFB. The LWA-SV DPS-4D was not transmitting but listening to the transmission from KAFB.

To maximize sensitivity to ionospheric reflections from nearby lightning strikes, we pointed a single beam near zenith, operating as a near-vertical incidence sounder. One tuning was set at a center frequency of 8 MHz (recording 3–13 MHz), and the other tuning was set at 74 MHz (recording 69–79 MHz). The reason for the 74 MHz tuning is made clear in the next section. These data are processed to form dynamic power spectra with 128, 78.125-kHz channels, retaining a time resolution of 12.8 μs.

3. Analysis Method

One lightning flash produces hundreds of broadband HF bursts during the breakdown process. These signals propagate outward in all directions. The ionosphere reflects frequencies below the maximum usable frequency back to Earth, imparting the tale-tell density profile dispersion of an ionogram. For nearby lightning an HF/VHF dipole receiver is capable of detecting both the direct line-of-sight signal as well as the dispersed ionospheric reflection. To ensure that no reflected signals corrupt the measurements of the direct line of sight, we set the higher tuning to a frequency well above the expected maximum usable frequency. However, since

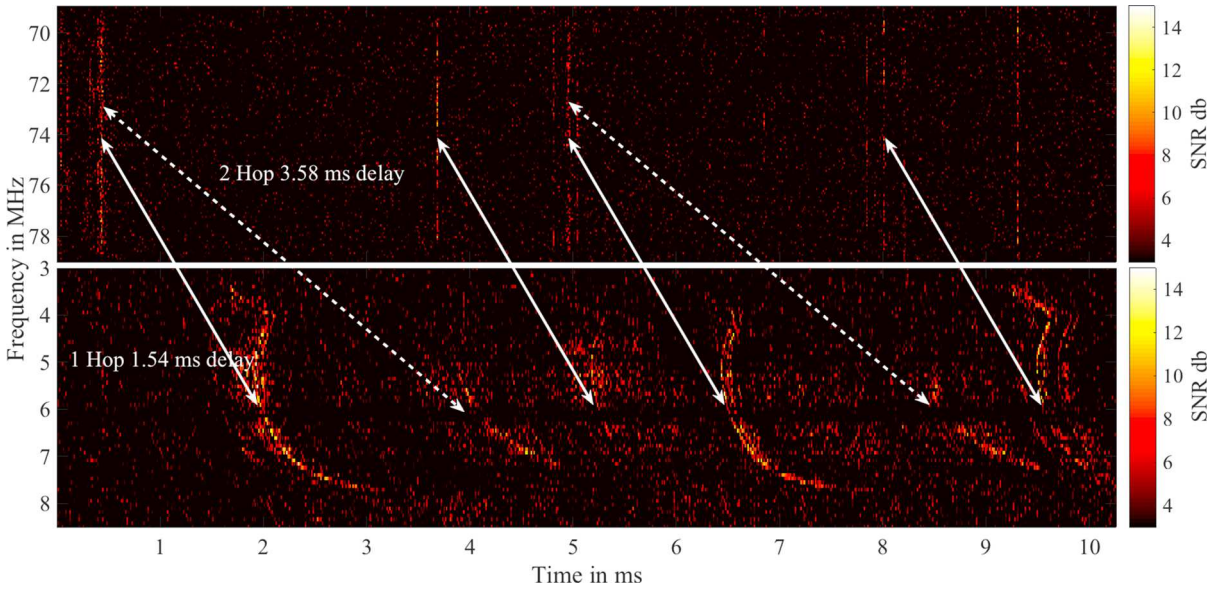

Figure 2. The very high frequency dynamic spectra of the direct line of sight (top) and the HF dispersed ionospheric reflection (bottom) of a few broadband radio bursts from a single lightning flash. The single hops (1.54 ms delay at 5 MHz) are marked with solid arrows, and double hops (3.84 ms delay at 5 MHz) are marked with dashed arrows. The HF dynamic spectra are shown for right-hand-circular (O mode) polarization. HF = high frequency; SNR = signal-to-noise ratio.

the beam was pointed near zenith, the VHF direct line-of-sight component was only detected through the beam side lobes. Despite this, lightning is so powerful at these frequencies it is still easily detectable.

Figure 2 shows an example dynamic power spectra of both the direct line of sight (approximately 74 MHz) and the ionospheric reflection (approximately 8 MHz) from a few bursts. For the bursts in Figure 2 it is easy to see both a single hop (source to ionosphere to receiver) delayed by 1.54 ms at 5 MHz and a double hop (source to ionosphere to ground to ionosphere to receiver) delayed by 3.58 ms at 5 MHz.

The time window shown in Figure 2 is relatively sparse with bursts and was chosen to show the fine detail of the measured bursts. For most lightning flashes there are typically hundreds to thousands of breakdown associated bursts packed within a few hundred milliseconds. While any of the bursts shown in Figure 2 could be used to create an ionogram alone, we can boost the SNR by combining many flashes together. This is accomplished by simply integrating the VHF (direct-line-of-sight) dynamic power spectra across frequency to form a high SNR power time series at the same sampling rate as the HF dynamic power spectra. We then cross correlate the VHF power time series with each frequency channel of the HF dynamic power spectra. The correlated power at a given delay as a function of frequency is effectively an ionogram. This process can only be done for one lightning flash at a time, since multiple flashes would result in a range smearing effect presuming they occurred at different locations.

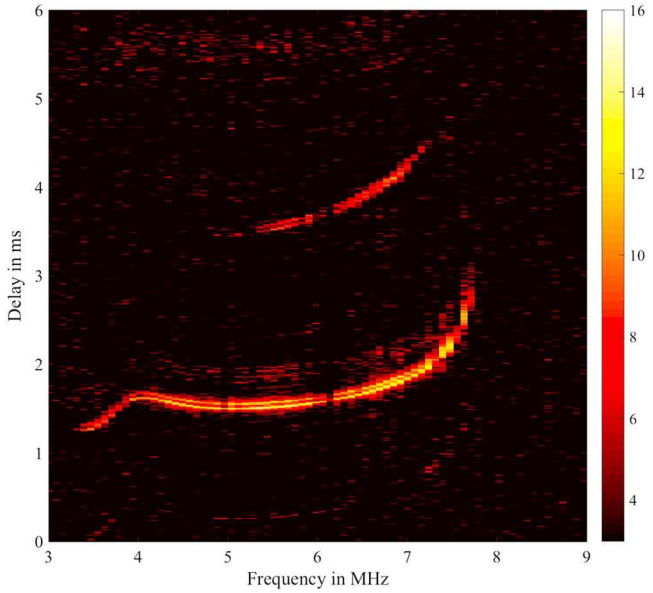

Figure 3. An O mode ionogram resulting from the correlation (amplitude only) of each 78.125-kHz channel from the HF ionospheric-reflection tuning with the averaged VHF direct-line-of-sight tuning. Note the bifurcation of the averaged trace by 52 μs in delay.

Figure 3 shows an example result of this correlation, where a single hop echo appears at a delay of 1.54 ms and the double hop at 3.58 ms at 5 MHz. The boost in signal to noise reveals that both the 1 and 2 hop echoes are actually composed of two parallel sweeps, separated by 52 μs. Such a feature is expected for IC lightning, since it occurs several kilometers above the ground, creating a cloud-to-ionosphere hop and cloud-to-ground-to-ionosphere hop. The timing of the lightning, had it occurred at the ground, is approximately the average timing between the two parallel sweeps. Under this interpretation, the 52-μs separation between the sweeps indicates that the lightning occurred 7.8 km above the ground, which is a reasonable value for IC lightning. The parallel sweep feature is present within all lightning flashes analyzed for this paper.

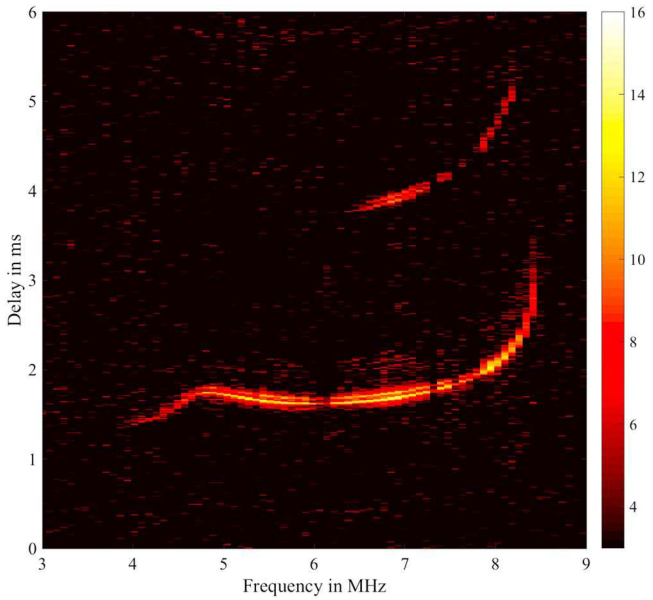

Figure 4. An X mode ionogram resulting from the correlation (amplitude only) of each 78.125-kHz channel from the high-frequency ionospheric-reflection tuning with the averaged very high frequency direct-line-of-sight tuning. Note the bifurcation of the averaged trace by 52 μs in delay.

We note that both O and X mode propagation are easily distinguished in our data by filtering with right-hand-circular (O mode) and left-hand-circular (X mode) polarizations. The data shown in Figures 2 and 3 are O mode, while Figure 4 shows the X mode correlated ionogram made for the same lightning flash as Figure 3.

The resultant ionogram from the amplitude correlation does not produce a true travel time; rather, it only provides the difference in travel time between the ionospheric reflection and direct line of sight. To calibrate the true travel time (lightning to ionosphere to receiver), we must know the distance x between the receiver and the lightning. An array with the ability to derive angle of arrival paired with a few outrigger antennas could use simple geometry and timing to solve for the distance. However, for this paper we only make use of a single beam; therefore, we developed a different method that uses the comparative timing of the single and double hop ionospheric echoes. The time delay for the single ionospheric hop echo can be expressed as $\tau_1 = \frac{R_1 - x}{c}$, where R_1 is the virtual path and c is the speed of light. Similarly, the time delay of the double hop echo is given by $\tau_2 = \frac{R_2 - x}{c}$. Approximating both the Earth and ionosphere as planar the virtual height of the ionosphere can be expressed as $H^2 = \frac{R_1^2}{4} - \frac{x^2}{4} = \frac{R_2^2}{16} - \frac{x^2}{16}$. Combining these expressions and solving for x in terms of τ_1 and τ_2 yields

$$x = \frac{c(4\tau_1^2 - \tau_2^2)}{2\tau_2 - 8\tau_1}. \quad (1)$$

In many cases, such as Figures 3 and 4, both the single and double hop echoes are detected, and we can therefore use equation (1) to approximate the distance to the lightning and thereby calibrate the ionogram. Figure 5 shows before and after calibration ionogram traces (O mode only) created using this technique on three different lightning flashes captured on 7 September 2017 at 23:37:07 (L1), 23:37:01 (L2), and 23:38:46 (L3) UTC to the nearest second. Calibrated distances for these three flashes are 71.4 (L1), 129.4 (L2), and 175.8 (L3) km. These ionograms are compared with traces derived from digisondes digisonde observations at KAFB and at LWA-SV and show good agreement after calibration. The KAFB trace is from the same ionogram shown in Figure 1.

The method laid out in this paper is summarized as follows:

1. A broadband receiver directly detects the VHF time series of a lightning flash (direct line of sight).
2. The receiver also detects the delayed/dispersed signal reflected from the ionosphere at HF.
3. The ionospheric component is then channelized to sufficiently small frequency bins (78.125 kHz for this paper).
4. The VHF direct line-of-sight time series is integrated or resampled to match the time sampling of each channel of the ionospheric component.
5. The VHF time series is correlated (amplitudes only) with each channel of the HF dynamic spectra.
6. The distance to the lightning is calculated using one of several estimation methods.
7. The correlated ionogram are shifted in time using the calculated time delay to the lightning.

4. Discussion

We have created the first ever ionograms using lightning as a signal source. This method is straight forward, requiring only a sensitive HF/VHF receiver along with relatively minimal data processing. The applications for such a system are widespread, opening new doors in ionospheric monitoring.

One such application arises from the fact that lightning often occurs in dispersed storm systems, with lightning flashes occurring in many locations in a short period of time. For instance, the three lightning ionograms shown in Figure 5 occur at different distances, meaning that three spatially separated points are measured. Further development could allow one receiver to probe spatial structure in the *E* and *F* regions such as patchy, sporadic *E* and TIDs. For instance, with dense enough storm activity, a well place receiver could make many

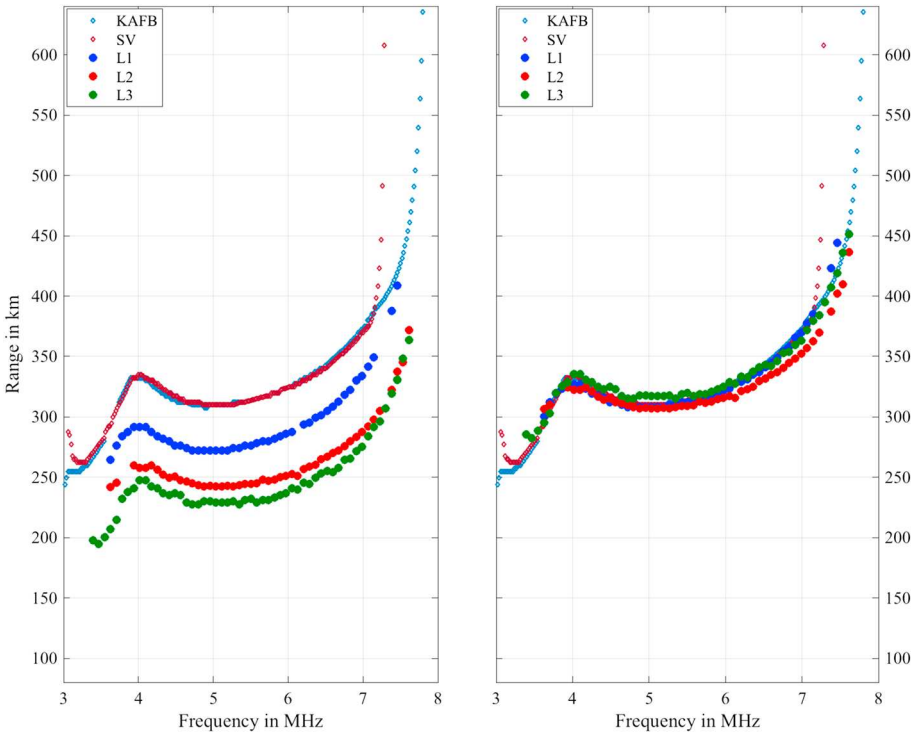

Figure 5. Plots comparing the ARTIST derived traces from the Kirtland Air Force Base (KAFB) and Sevilleta (SV) digisondes (blue and red diamonds) captured on 7 September 2017 at 23:43 UT. Also shown are lightning captured ionograms (blue, red, and green dots) captured just a few minutes before the digisonde captures. The left panel shows the lightning ionograms before the two hop calibration, and the right panel shows them after two hop calibration. The calibrated distances derived for these three flashes are 71.4 (L1), 129.4 (L2), and 175.8 km (L3).

ionograms over a broad region, potentially Nyquist sampling TIDs in the region. Such observations would allow for three-dimensional imaging of TID wavefronts.

This method also allows observations in restricted frequency bands that are off limits to standard transmit/receiver systems. Crucial ionospheric frequencies, such as foF1 and foF2, can often lie within protected frequency bands. Under such conditions accurate ionospheric specification is difficult and occasionally not possible with a standard HF sounder. Lightning, of course, is not subject to frequency allocation laws, meaning it can provide frequency fidelity where other transmitters cannot. For the KAFB ionogram shown in Figure 1, foF2 was within the 7.2–7.8 MHz protected band, which makes autoscaling more difficult.

Acknowledgments
This research was funded in part by the Air Force Office of Scientific Research (AFOSR). Construction of the LWA has been supported by the Office of Naval Research under Contract N00014-07-C-0147 and by the AFOSR. Support for operations and continuing development of the LWA1 is provided by the Air Force Research Laboratory and the National Science Foundation under grants AST-1711164 and AGS- 1708855. All of the LWA-SV data used in this article are publicly available at the LWA Data Archive (http://lda10g.alliance.unm.edu).

References

Cranmer, M. D., Barsdell, B. R., & Price, D. C. (2017). Bifrost: A Python/C++ framework for high-throughput stream processing in Astronomy. *JAI*, *6*(4), 1750007.

Cummer, S. A., Inan, U. S., & Bell, T. F (1998). Ionospheric *D* region remote sensing using VLF radio atmospherics. *Radio Science*, *33*(6), 1781–1792.

Ellingson, S. W., Taylor, G. B., Craig, J., Hartman, J., Dowell, C. N., Wolfe, T. E., et al. (2013). The LWA1 radio telescope. *IEEE Transactions on Antennas and Propagation*, *61*(5), 2540–2549.

Jacobson, A. R., Holzworth, R., Lay, E., Heavner, M., & Smith, D. A (2007). Low-frequency ionospheric sounding with narrow bipolar event lightning radio emissions: Regular variabilities and solar-X-ray responses. *Annales Geophysicae*, *25*, 2175–2184.

Jacobson, A. R., Holzworth, R., & Shao, X.-M (2008). Low-frequency ionospheric sounding with narrow bipolar event lightning radio emissions: Energy-reflectivity spectrum. *Annales Geophysicae*, *26*, 1793–1803.

Proctor, D. E. (1981). VHF radio pictures of lightning flashes to ground. *Journal of Geophysical Research*, *86*, 4041–4071.

Proctor, D. E., Uytenbogaardt, R., & Meredith, B. M (1981). VHF radio pictures of cloud flashes. *Journal of Geophysical Research*, *86*, 4041–4071.

Reinisch, B. W., Galkin, I. A., Khmyrov, G. M., Kozlov, A. V., Lisysyan, I. A., Bibl, K., et al. (2008). Advancing digisonde technology: The DPS-4D. In P. Song (Ed.), *Radio Sounding and plasma physics, American Institute of Physics Conference Series* (Vol. 974, pp. 127–143). Lowell, MA.

Reinisch, B. W., & Huang, X. (1983). Automatic calculation of electron density profiles form digital ionograms. 3: Processing of bottom side ionograms. *Radio Science*, *18*, 447–492.

Rhodes, C. T., Shao, X.-M., Krehbiel, P. R., Thomas, R. J., & Hayenga, C. O (1994). Observations of lightning phenomena using radio interferometry. *Journal of Geophysical Research*, *99*, 13,059–13,082.

Rison, W., Thomas, R. J., Krehbiel, P. R., Hamlin, T., & Harlin, J. (1999). A GPS-based three-dimensional lightning mapping system: Initial observations in central New Mexico. *Geophysical Research Letters*, *26*, 3573–3576.

Shao, X. M., & Krehbiel, P. R. (1996). The spatial and temporal development of intracloud lightning. *Journal of Geophysical Research*, *101*, 26,641–26,668.

Shao, X. M., Krehbiel, P. R., Thomas, R. J., & Rison, W. (1995). Radio interferometric observations of cloud-to-ground lightning phenomena in Florida. *Journal of Geophysical Research*, *100*, 2749–2783.

Shao, X.-M., & Rhodes, C. T (1996). Broad band radio interferometry for lightning observations. *Geophysical Research Letters*, *23*(15), 1917–1920.

Thomas, R. J., Krehbiel, P. R., Rison, W., Hunyady, S. J., Winn, W. P., Hamlin, T., & Harlin, J. (2004). Accuracy of the lightning mapping array. *Journal of Geophysical Research*, *109*, D14207. https://doi.org/10.1029/2004/JD004549